

Accelerated durability assessment of motorcycle components in real-time simulation testing

K-Y Lin^{1,2}, J-R Hwang^{1*}, and J-M Chang²

¹Department of Mechanical Engineering, National Central University, Jhongli, Taiwan, Republic of China

²Department of Component Quality, Automotive Research and Testing Center, Lugang, Changhua, Republic of China

The manuscript was received on 4 November 2008 and was accepted after revision for publication on 21 July 2009.

DOI: 10.1243/09544070JAUTO1059

Abstract: The rapid development of the vehicle industry has made reducing product development time a major concern. This study seeks to identify a suitable accelerated approach to durability analysis for motorcycle components. This investigation involves field data acquisition, laboratory road load simulation, accelerated durability testing, and fatigue life prediction. Two methods, 'strain range editing technique' and 'racetrack editing technique', were applied to edit field strain histories for accelerated durability tests. Furthermore, four methods, including the 'S-N approach with fatigue property of base metal', 'Eurocode 3 approach', 'BS 5400 approach', and 'BS 5400 approach with Gurney thickness modification', were employed to assess fatigue life. Three road types and four damage levels were also used. The results demonstrated that the 'BS 5400 approach with Gurney thickness modification' is a suitable method of assessing the durability of welded motorcycle components when the fatigue properties of critical points are not available. Both the 'strain range editing technique' and 'racetrack editing technique' can effectively edit strain histories with the expected quantity of fatigue damage, and demonstrate satisfactory agreement between the experimental data and predicted data.

Keywords: motorcycle component, accelerated durability assessment, signal condensation, road load simulation

1 INTRODUCTION

Because of the rapid development of the vehicle industry, cost reduction and shortening of product development time have become key subjects. One of the methods achieving these objectives is the accelerated durability analysis and testing based on fatigue theory [1, 2]. Durability test is an important task for design verification. The challenge faced by engineers in the vehicle industry is how to design an accelerated durability test in the laboratory. The laboratory durability testing must be accelerated in order to reproduce the desired amount of fatigue damage in a short time; then the cost reducing and time saving could all be achieved at the same time.

In addition, the application of closed-loop servo-hydraulic testing systems and the road simulation technique has enabled the reproduction of test track responses such as displacement, acceleration, and strain in the laboratory [3–6]. Simulated laboratory durability testing, test track durability testing, and proving-ground durability testing can be performed simultaneously. These methods provide significant input to final product decisions.

Accelerated durability testing can be employed to minimize testing time and cost, which was based on cumulative fatigue damage theory [7] and the equivalent fatigue damage calculation method. Dowling [8] presented a method based on equivalent fatigue damage calculation for data correlation. Furthermore, Jeong *et al.* [9] proposed the laboratory simulation technique for accelerating component durability testing using a multiaxial simulation table, and reduced the test time to $\frac{1}{4}$. Additionally, Su *et al.* [10] presented an accelerated test procedure to

*Corresponding author: Department of Mechanical Engineering, National Central University, Jhongli, Taiwan 32001, Republic of China.

email: jrhwang@ncu.edu.tw

reduce the component durability test time, which was based on the computer aided engineering (CAE) equivalent fatigue damage technique. Moreover, Ledesma *et al.* [11] devised the accelerated durability testing schedule for the multi-axis suspension system, which correlates with customer usage, and is based on equivalent fatigue damage calculation. A methodology for physical test optimization based on vehicle suspension, chassis, and body was presented [12], and the road load history was edited for the component bench durability test, which was based on fatigue damage analysis. Panse and Awate [13] devised an accelerated structure durability testing programme and applied it to complete vehicles and components according to customer usage. This approach was also based on the equivalent fatigue damage correlation method.

Three common methods exist for accelerating testing, including 'increasing testing frequency', 'using higher testing load', and 'eliminating numerous small load cycles from the load spectrum'. All three of these methods have significant advantages of lower test time and cost, but each also has disadvantages. Increased frequency may have an effect on lifetime, possibly resulting in inadequate time for the full operation of environmental aspects. Increasing loads beyond service loads results in accelerated tests but can yield misleading results; residual stresses that might have remained in service may be changed by excessive test loads. It is common for many small load cycles to be eliminated from the test load spectrum, and various analytical methods exist to help eliminate low-damaging cycles; such methods may hide the influences of both fretting and corrosion.

Laboratory simulation methods can produce virtually any prescribed sequence of load, acceleration, displacement, or strain. Test time and cost can be reduced via a condensed version of the real history. Condensed histories include selected peaks and valleys in their real sequence and omit many small peaks and valleys. The most significant peaks and valleys can be selected by editing a rainflow [14] count to retain only the largest ranges of data. Conle and Topper [15] utilized a technique involving the editing of service strain history to omit strain cycles below various gate levels and to assess damage. Canfield and Villaire [16] developed a method of accelerated component durability testing, which involved the removal of cycle regions that did not cause significant component damage. Additionally, Sharp *et al.* [17] applied the accumulated damage method to reduce the multi-axis road load data of

the bench testing, which was edited to reduce the test time while maintaining as much accumulated damage as possible. Khosrovaneh *et al.* [18] discussed different methods of accelerating fatigue analysis, including time history reduction (peak-valley counting) and the element elimination technique (removal of low-damage elements). Furthermore, two methods, including the 'strain range editing technique' [19] and the 'racetrack editing technique' [20], were also applied to edit service strain histories for accelerated durability tests.

The fatigue design methodologies for metallic components have traditionally been based on the stress-life (S-N) approach. This approach works well for the high cycle fatigue (HCF) problem, while the strain-life (ϵ -N) approach focuses on the low cycle fatigue (LCF) problem. Fatigue cracks affecting motorcycle components generally occur in the welded regions. It is necessary to identify the most appropriate fatigue analysis approach for specific problems. Numerous reasons exist for reduced fatigue strength in welded structures, including global stress concentration, residual stresses, weld flaws, and the heat affected zone. A statistical analysis of fatigue tests on steel welded structures was performed in 1972 [21], and led to the development of fatigue design for welded structures, something that has now been incorporated into many standards. The BS 5400 standard [22] has been applied to predict welded structure fatigue life for many years, while the Eurocode 3 standard [23] is a new one. When considering the thickness effect, the damage model can be modified using the Gurney equation [24]. Additionally, other standards exist for obtaining S-N curves of welded structures, including AASHTO [25], AISC [26], API RP2A [27], AREA [28], AWS: PT9 [29], and ARSEM [30].

Previous studies have demonstrated that the S-N method is more easily and widely used than the ϵ -N method in the event of cracks occurring near the welded regions. This explains the difficulty in obtaining the input parameters of the ϵ -N method, including fatigue properties, stress concentration factor, residual stress, and so on. The S-N method has been included in many codes for the fatigue design of welded structures [22, 23, 25-30]. This study seeks to identify a suitable accelerated durability analysis approach for motorcycle handlebars. The proposed procedure comprises field data acquisition, road load simulation, experimental design, the accelerated durability test, and fatigue life prediction. Two methods, including the 'strain range editing technique' and 'racetrack editing technique',

were applied to edit field strain histories for accelerated durability tests. Furthermore, four methods, including the 'S-N approach with fatigue property of base metal', 'Eurocode 3 approach', 'BS 5400 approach', and 'BS 5400 approach with Gurney thickness modification', were employed to analyse handlebar fatigue life. Additionally, three road types and four damage levels were conducted.

2 THEORY

2.1 Fatigue life evaluation of welded structure

Fatigue life of welded structures may be influenced by geometric shape, material property, residual stresses, weld defects, and so on. Owing to these complexities, fatigue design for welded structures is much more difficult than for non-welded metals. After reviewing the statistical analysis of published fatigue data, fatigue design rules for welded structures have been developed extensively during the last 30 years. Initial efforts were focused on steel bridges, and the rules laid out in BS 5400 evolved from data published by the British Standards Institution.

2.1.1 BS 5400 [22]

The Part 10 standard formulated by the British Standards Institute was developed to assess the fatigue life of steel, concrete, and composite bridges. Nine classes of welded details were classified according to load type, location of potential crack initiation, weld geometry, and so on. The classes were classified as follows: class B, class C, class D, class E, class F, class F2, class G, class S, and class W. In references [31] and [32], the method for classifying welded details based on this standard was rearranged and tabulated in a convenient form together with corresponding schemes and legends illustrating the data clearly and concisely.

The parameters describing the median S-N curve and standard deviation of each class based on the assumption of the lognormal distribution of fatigue life are listed in the BS 5400 standard to provide a design reference. Therefore, it can provide a method for predicting fatigue life with various failure probabilities.

When $N_f \leq 10^7$, the correlation between fatigue life and nominal stress is

$$\log N_f = \log K - z\sigma - m \log S_n \quad (1)$$

where

N_f = fatigue life

K = constant related to the median line of the statistical analysis results

z = number of standard deviations below the median line

σ = standard deviation of $\log N_f$

m = inverse slope of the median line ($(\log S_n) - (\log N_f)$) curve

S_n = nominal stress range

When $N_f > 10^7$, the equation is

$$\log N_f = \log K - z\sigma - (m+2) \log S_n \quad (2)$$

Because the thickness of welded structure influences the fatigue strength, this study uses the thickness modification approach of Gurney [24, 32] and compares it with the other approaches used in this study. The Gurney modification equations are as follows

When $N_f \leq 10^7$

$$\log N_f = \log K - z\sigma - m \log \frac{S_n}{(22/t)^{0.25}} \quad (3)$$

When $N_f > 10^7$

$$\log N_f = \log K - z\sigma - (m+2) \log \frac{S_n}{(22/t)^{0.25}} \quad (4)$$

In addition, the S-N curve of base metal (JIS S25C carbon steel) was obtained from a series of fully reversed bending fatigue tests. The testing method and specimen dimensions all followed the JIS z2275 standard.

Data required in the fatigue analysis include:

- load history: nominal stress history (= Young's modulus \times nominal strain history);
- welded detail class;
- thickness of the welded structure;
- material properties (S-N curve);
- failure probability (= 50 per cent in this study).

2.1.2 Eurocode 3 [23]

Design of steel structures – Parts 1 to 9: Fatigue (BS EN 1993-1-9) will partially supersede BS 5400 standard – Part 10, and was published by the British Standards Institute on 18 May 2005. Fourteen categories of welded details were classified according to load type, location of potential crack initiation,

weld geometry, and so on. The detail categories were classified as follows: 36, 40, 45, 50, 56, 63, 71, 80, 90, 100, 112, 125, 140, and 160 N/mm². The fatigue strength for the nominal stress range is represented by a series of $(\log S_n) - (\log N_f)$ curves, which correspond to typical detail categories. Each detail category is designated by a number which represents, in N/mm², the reference value σ_C for the fatigue strength at 2 million cycles.

For nominal stress spectra with stress ranges above and below the constant amplitude fatigue limit σ_D , the fatigue strength should be based on the extended fatigue strength curves as follows

When $m = 3$ and $N_f \leq 5 \times 10^6$, the equation is

$$S_n^m \times N_f = \sigma_C^m \times (2 \times 10^6) \quad (5)$$

When $m = 5$ and $5 \times 10^6 \leq N_f \leq 10^8$, the equation is

$$S_n^m \times N_f = \sigma_D^m \times (5 \times 10^6) \quad (6)$$

where

σ_C = detail category, or the fatigue strength at 2 million cycles

σ_D = constant amplitude fatigue limit, or the fatigue strength at 5 million cycles

m = inverse slope of the median line ($[\log S_n] - [\log N_f]$) curve

2.2 Road load simulation technique

This technique can rapidly reproduce the road load and failure mode in a laboratory and verify the structural durability of the target component or complete vehicle. Figure 1 shows the flowchart of the road load simulation technique. The iteration process is summarized as follows.

First, the target signal $\{y(t)\}$ is converted to $\{Y(f)\}$ via the fast Fourier transformation (FFT); then it is timed with the inverse function of the transfer function (IFFT) $[G(f)]^{-1}$ to obtain $\{X(f)\}_{(0)}$; finally, the inverse function is obtained and a factor k is timed to become the initial drive file $\{x(t)\}_{(0)}$, as shown by

$$\{x(t)\}_{(0)} = k \times \text{IFFT} \left[\{G(f)\}^{-1} \{Y(f)\} \right] \quad (7)$$

Following activation with the drive file $\{x(t)\}_{(n)}$, the response data $\{y(t)\}_{(n)}$ can be measured, thus enabling the new drive file to be modified by com-

paring the deviation of the target data $\{y(t)\}$ and response data $\{y(t)\}_{(n)}$. These processes are then repeated until the error has converged to a reasonable range, where $\{x(t)\}_{(n)}$ is the drive file and $\{y(t)\}_{(n)}$ is the response data

$$\{E(f)\}_{(n)} = \text{FFT} \left[\{y(t)\} - \{y(t)\}_{(n)} \right] \quad (8)$$

The correction item is

$$\{c(t)\}_{(n)} = \text{IFFT} \left[\{G(f)\}^{-1} \{E(f)\}_{(n)} \right] \quad (9)$$

The new drive file is

$$\{x(t)\}_{(n+1)} = \{x(t)\}_{(n)} + k \times \{c(t)\}_{(n)} \quad (10)$$

with re-drive $\{x(t)\}_{(n+1)}$ and re-measure $\{y(t)\}_{(n+1)}$, where (n) denotes the repeated number and k represents the proportion factor.

2.3 Signal condensation

Several techniques exist for accelerated durability testing including the frequency accelerated method, stress increased method, signal condensed method, and damage equivalent method. The frequency accelerated method increases the operating frequency, or uses a continuous action to reduce the testing period. Meanwhile, the stress increased method multiplies the input stress, causing rapid failure of the target specimen. Moreover, the signal condensed method eliminates the non-damage signal history, in order to shorten the input signal history and accelerate the durability testing. The damage equivalent method employs the fatigue life evaluation technique, and effectively accelerates the duration time. This study focuses on the signal condensed methods, including the strain range editing and racetrack editing techniques.

2.3.1 Strain range editing technique

The strain range editing method employs a peak-to-peak strain range value (namely threshold) for editing. Strain histories smaller than the preset threshold value are removed.

2.3.2 Racetrack editing technique

The racetrack editing method is shown in Fig. 2. The original history in Fig. 2(a) is condensed to that in

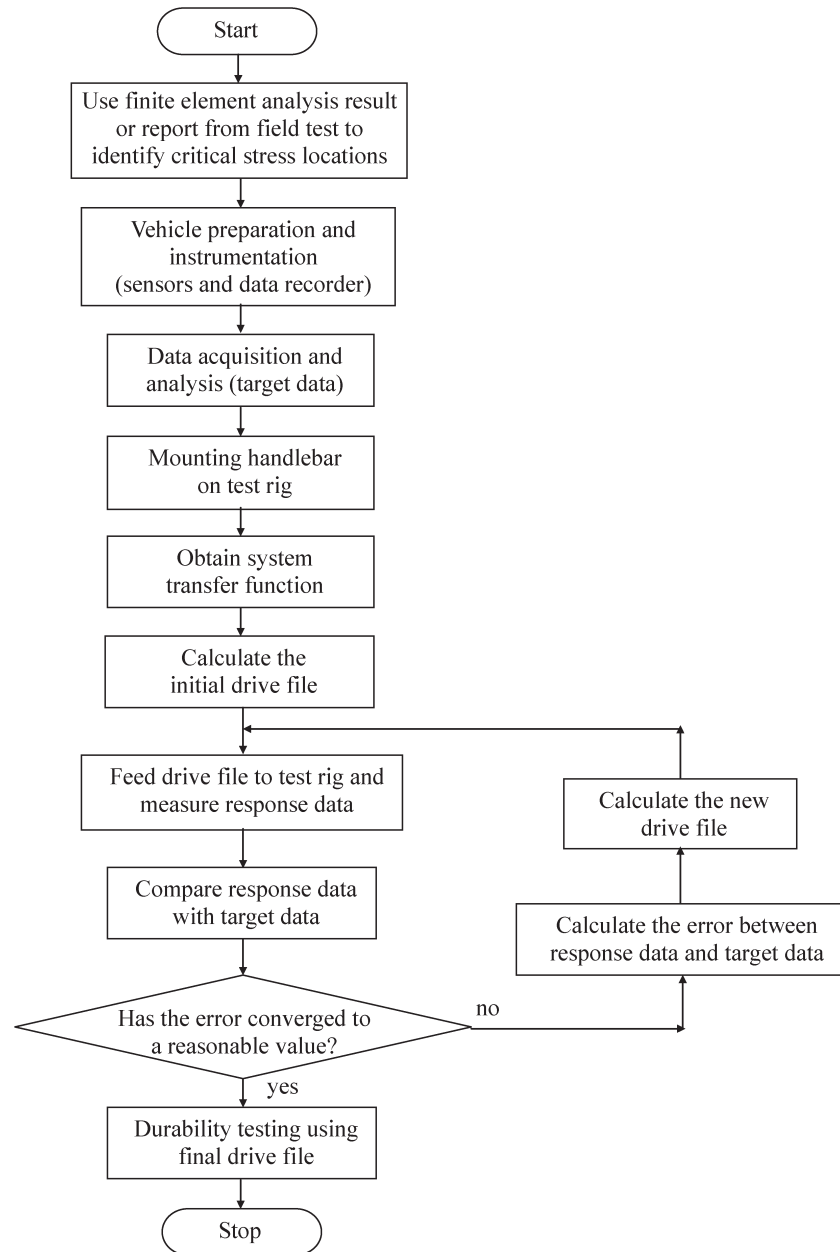


Fig. 1 Flowchart of road load simulation technique

Fig. 2(c). The method used to eliminate smaller ranges is shown in Fig. 2(b), and the ‘racetrack’ of width s (namely the gate value) is defined, bounded by ‘fences’ exhibiting the same profile as the original history. The condensed history includes the sequence of events, which may be important. This method is useful for condensing histories to those few events, perhaps 10 per cent of the total, that are most damaging, and which generally account for over 90 per cent of all calculated damage. The condensed histories accelerate test time and permitted attention to be focused on a few significant events.

3 METHODS

This study conducted data acquisition, road load laboratory simulation, signal condensation, fatigue life evaluation, and durability tests. The experimental procedures and methods were as follows.

3.1 Target component and target road

The target vehicle used in this study was a 150 cm³ motorcycle, the handlebar of which was the target component (shown in Fig. 3). The target roads were a Belgian road (paved road), uneven asphalt road,

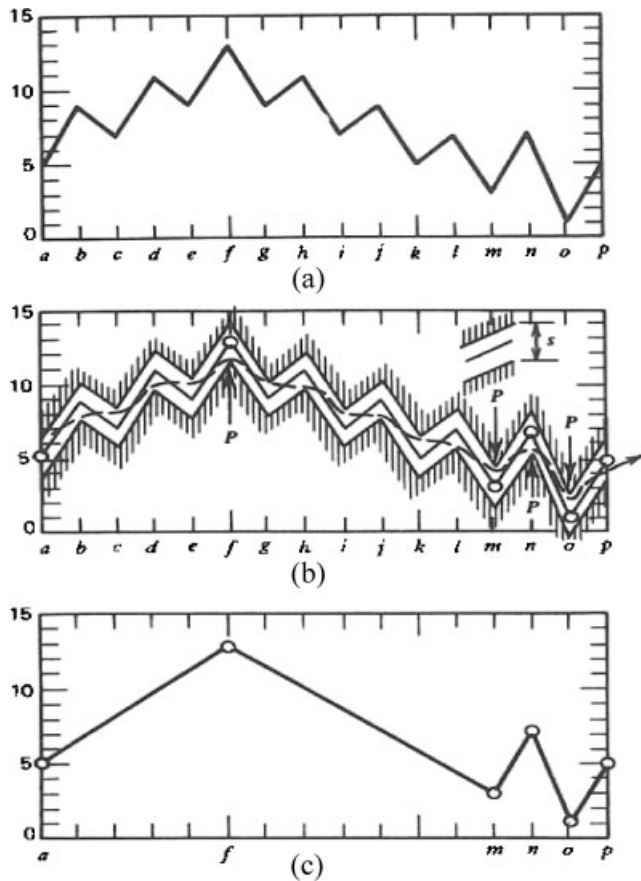


Fig. 2 Example of the racetrack editing method: (a) an irregular history; (b) screening through width s ; (c) the resulting condensed history [20]

and non-uniform-hole road at the proving ground in the ARTC (Automotive Research and Testing Center in Republic of China).

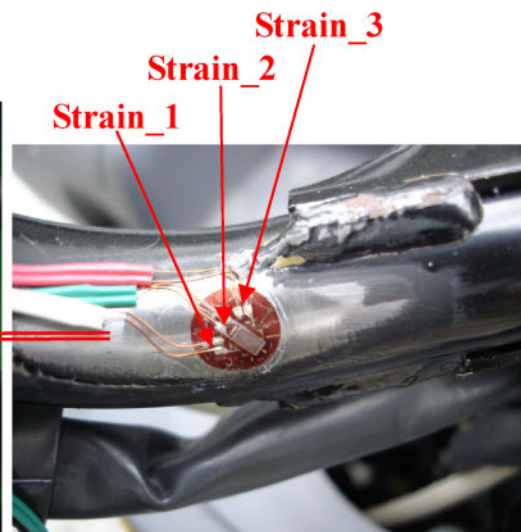
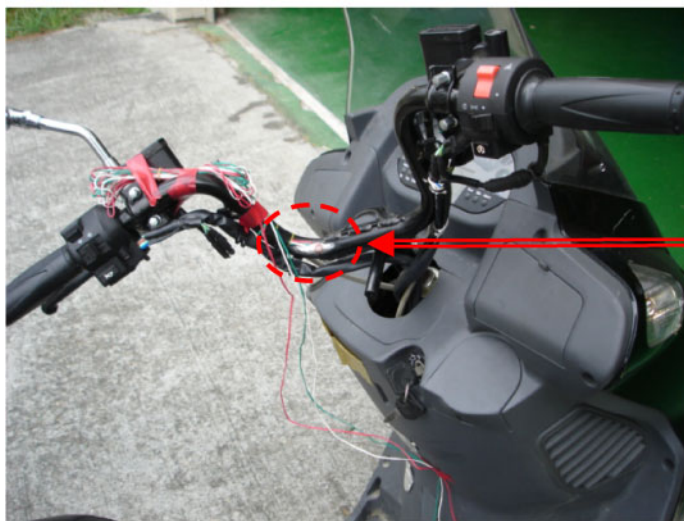


Fig. 3 Target component (motorcycle handlebar) and the strain gauge location

3.2 Data acquisition on proving ground

The motorcycle was driven on the Belgian road at a speed of 30 km/h, uneven asphalt road at 40 km/h, and non-uniform-hole road at 60 km/h. The three-axis rosette strain gauges (KYOWA, 350 Ω , gauge length 3 mm) were used for the tests (shown in Fig. 3). A data recorder (IMC-CRONOS) was mounted at a suitable location on the test vehicle. The sampling rate was 1000 Hz. Strain histories of the handlebar were measured and edited to ensure good data quality and freedom from spikes, noise, and so on.

3.3 Experimental design

Pilot fatigue analysis revealed that the fatigue lives of the original field strain histories ($\times 1$ magnification) did not cause handlebar cracking. Therefore, the original field strain histories were multiplied by six and became the target strain signals ($\times 6$ magnification). Additionally, this study aimed to evaluate the influence of these three parameters, including the different levels of retained damage, road types, and signal condensation methods. These parameters are described below, and Table 1 lists the identification information and acceleration factor of these durability tests. Eleven specimens were tested based on the edited loading histories for different damage levels, road types, and signal condensation methods.

1. Damage retained levels: 100, 70, 50, and 30 per cent are shown in case 1 to case 4 of Table 1.

Table 1 The identification and acceleration factor of durability tests

Case number	Signal condensation method	Road type	Damage retained (%)	Gate value (%)	Threshold of strain range ($\mu\epsilon$)	Original record	Retained reversals	Acceleration factor
1	Racetrack editing	Belgian road	100	0.0		81 052	2212	1
2	Racetrack editing	Belgian road	70	20.5		81 052	318	7
3	Racetrack editing	Belgian road	50	29.0		81 052	188	12
4	Racetrack editing	Belgian road	30	39.5		81 052	94	24
5	Racetrack editing	Uneven asphalt road	100	0.0		31 084	712	1
6	Racetrack editing	Uneven asphalt road	70	20.0		31 084	64	11
7	Racetrack editing	Non-uniform-hole road	100	0.0		15 442	400	1
8	Racetrack editing	Non-uniform-hole road	70	30.0		15 442	32	13
9	Strain range editing	Belgian road	70		830	81 052	268	8
10	Strain range editing	Belgian road	50		1185	81 052	126	18
11	Strain range editing	Belgian road	30		1700	81 052	42	53

- Road types: Belgian road, uneven asphalt road, and non-uniform-hole road are shown in cases 1, 5, 7 (100 per cent damage retained level) and cases 2, 6, 8 (70 per cent damage retained level) of Table 1.
- Signal condensation methods: two techniques are included here, the 'racetrack editing method' and the 'strain range editing method'. These two techniques are presented in cases 1 to 4 and cases 9 to 11 of Table 1 respectively.

3.4 Road load simulation durability tests

Fixtures required for accelerated durability tests were designed and manufactured. The 'strain_1' component was considered to simulate the road load in this study (shown in Fig. 3). The edited strain histories, including different damage levels, road types, and signal condensation techniques, were reproduced in the laboratory using a remote parameter control technique to derive the applied loading history (final drive file) with a single servo-hydraulic actuator in the durability test, which is shown in Fig. 4.

3.5 Accelerated durability test

Four damage levels, three road types and two signal condensation techniques of loading histories obtained from road load simulation were applied in the durability tests (from case 1 to case 11 of Table 1). Furthermore, periodic inspection was performed to identify crack initiation (2.5 mm).

3.6 Fatigue life evaluation

The S-N approach, rainflow cycle counting method, Miner damage accumulation rule, Eurocode 3

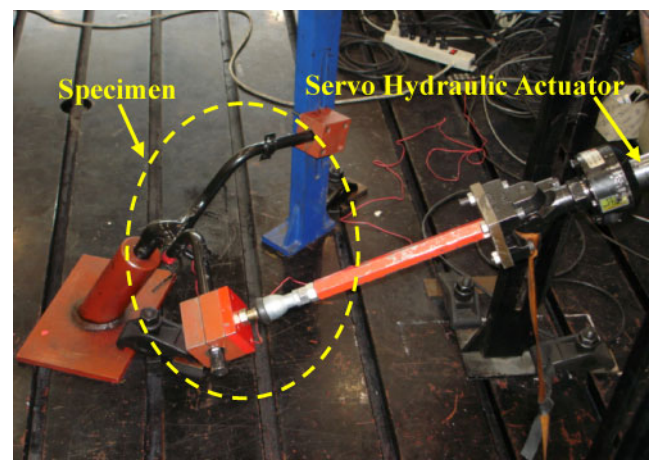


Fig. 4 Set-up condition of the accelerated durability test and the target specimen

standard, BS 5400 standard, and Gurney thickness modified equation were employed for fatigue life evaluation [33]. Comparison between the experimental and predicted fatigue lives of motorcycle handlebars subjected to full length and edited histories, including three road types and four damage levels, were employed to evaluate the effect of these two signal condensation techniques.

4 RESULTS AND DISCUSSION

This section demonstrated the results of accelerated durability analysis and road load simulation accelerated durability tests. The experimental and predicted fatigue lives were also compared for all cases. The results are discussed in detail below.

4.1 Fatigue life evaluation

This study did not use the ϵ -N approach because it requires the estimation of several input parameters,

including fatigue properties of the heat affected zone and weld metal, stress concentration factor, residual stress, etc. The need for such estimation makes the method vulnerable to inaccurate prediction. The S–N method has been included in many codes for fatigue design of welded structures [22]. Previous studies have demonstrated that the S–N method is more easily and widely used than the ϵ –N method in the event of cracks occurring near welded regions.

Since fracture of the handlebar occurs near the welded region, it is necessary to consider the welded effect in predicting fatigue life. Four methods, including the ‘S–N approach with fatigue property

of base metal’, ‘Eurocode 3 approach’, ‘BS 5400 approach’, and the ‘BS 5400 approach with Gurney thickness modification’, were used to predict handlebar fatigue lives in accelerated durability tests. The welded details were classified respectively as: detail category 80 based on Table 8.5 of the Eurocode 3 standard: Parts 1–9, and G class based on the BS 5400 standard: Part 10; these are illustrated in Figure 5. Figure 6 shows the S–N curves obtained from the bending fatigue test of base metal, Eurocode 3 (detail category 80), BS 5400 (G class), and BS 5400 (G class) with the Gurney thickness modification respectively. The material properties of the

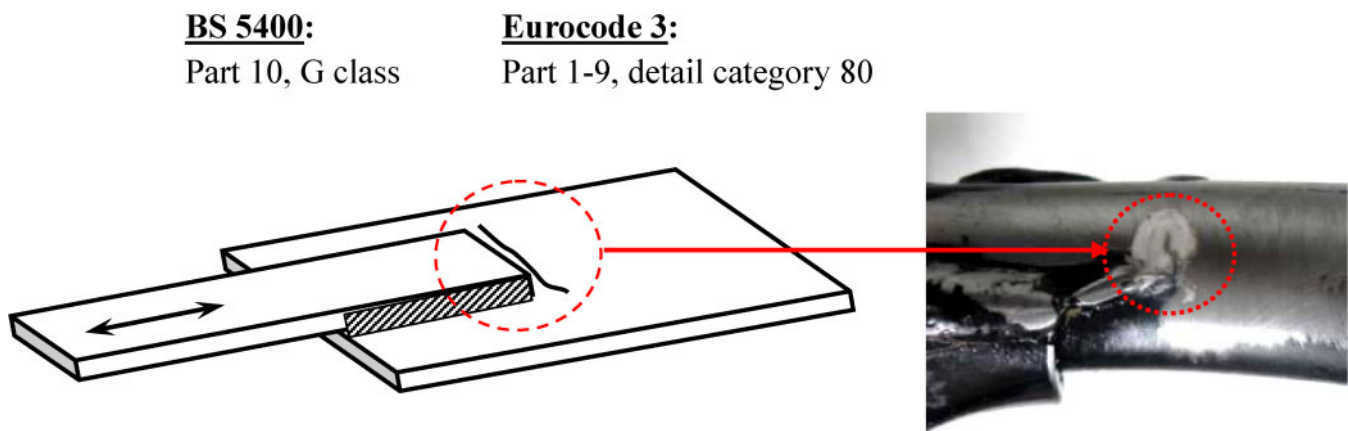


Fig. 5 Fracture location at welded region, the detail category 80 of Eurocode 3 standard, and the G class of BS 5400 standard (classification of details are from references [22] and [23])

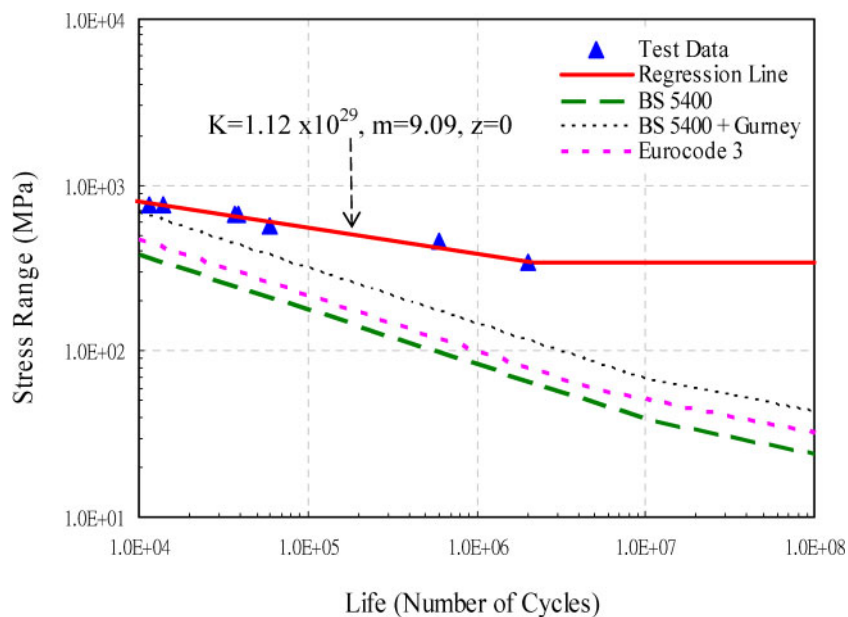


Fig. 6 Stress–life curve of test data, Eurocode 3 (detail category 80), BS 5400 (G class), and BS 5400 (G class) with Gurney thickness modified equation

Table 2 Comparison of the fatigue lives for the motorcycle handlebar

Case number	Predicted life (blocks)				Experimental life (blocks)	Factor*
	S-N approach with fatigue properties of base metal	Eurocode 3 standard	BS 5400 standard ($t = 22$ mm)	BS 5400 with Gurney thickness modification ($t = 2.3$ mm)		
1	2370	145	81	441	763	1.73
2	2638	208	116	633	905	1.43
3	2741	293	163	887	1364	1.54
4	2934	480	267	1455	2193	1.51
5	36801	1130	629	3427	6950	2.03
6	43507	1602	892	4849	13178	2.72
7	4825	508	283	1541	2682	1.74
8	6971	724	403	2194	4350	1.98
9	2638	208	116	629	1023	1.63
10	2741	289	161	876	1548	1.77
11	2934	487	271	1476	2482	1.68

*Factor = experimental life/predicted life (BS 5400 with Gurney thickness modification).

handlebar are as follows: ultimate strength 420 MPa, yield strength 395 MPa, Young's modulus 210 GPa, and strain_1 component was considered to evaluate nominal stress range S_n . The parameters describing the median S-N curve of base metal are $K = 1.12 \times 10^{29}$ and $m = 9.09$. Parameters describing the S-N curve of the G class detail in equations (1) and (2) are $K = 5.7 \times 10^{11}$, $\sigma = 0.662$, and $m = 3.0$ respectively. The median fatigue life is predicted using $z = 0$ in this study. Parameters describing the S-N curve of the detail category 80 in equations (5) and (6) are $\sigma_C = 80.0$, $\sigma_D = 58.9$, and $m = 3.0$ respectively.

Table 2 lists the experimental fatigue lives and the fatigue lives predicted using four theoretical methods (1 block = 1 trip for each road). The results of the S-N approach with fatigue property of base metal significantly exceed the experimental results (ranged from 1.18 to 5.30), indicating that weld quality influences the fatigue life and that the stress concentration effect of the weld toe should be considered. The results of the Eurocode 3 approach were lower than those of experiments, where the difference ranged from 4.35 to 8.23. The BS 5400 approach obtained lower lives than those of experiments, because the original information for the BS 5400 standard was obtained using a weld with 22 mm thickness. When the thickness decreases, the specimen tends to lead to conservative fatigue life predictions. On the other hand, the BS 5400 approach with the Gurney thickness modification (thickness of 2.3 mm, the same as the handlebar) gives a satisfactory result. The differences between the prediction and experiment results are within the acceptable range of 3 times, indicating that the third approach (BS 5400 approach with Gurney thickness modification) could satisfactorily assess the structure durability of the motorcycle handlebar.

4.2 Road load simulation and failure mode

The applied loading histories in durability tests were obtained using the remote parameter control technique based on the reproduction of the strain histories of the motorcycle handlebar. The target strain histories measured using the Belgian road ($\times 6$ magnification) were reproduced in the laboratory. The error between the target r.m.s. (root mean square) strain and response history was less than 10 per cent for all durability tests. Table 3 summarizes these results. Figure 7 shows the failure mode for the accelerated durability tests. The failure modes among different signal condensation methods, different damage retained levels, and different road types were almost the same, and all occurred where the handle was welded to the main pipe.

4.3 Accelerated durability assessment

Two methods, including the 'strain range editing technique' and 'racetrack editing technique', were employed to edit the strain histories for the accelerated

Table 3 The results of road load simulation tests

Case number	Target r.m.s.* strain ($\mu\epsilon$)	Response r.m.s. strain ($\mu\epsilon$)	Error (%)
1	414.0	409.0	1.21
2	608.0	552.2	9.18
3	708.0	671.3	5.18
4	601.0	558.4	7.09
5	406.0	370.2	8.82
6	499.2	458.2	8.21
7	656.6	625.3	4.77
8	732.3	701.1	4.26
9	686.0	651.4	5.04
10	731.0	692.5	5.27
11	864.0	808.1	6.47

*Root mean square.

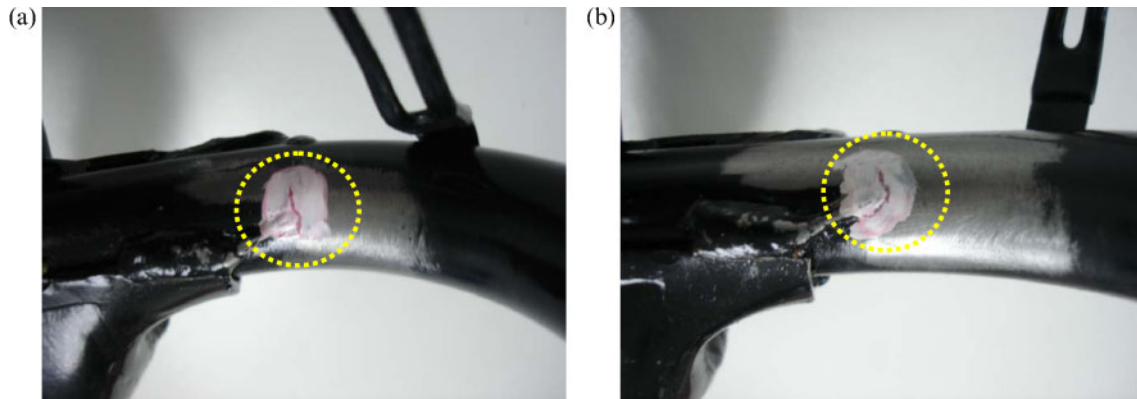


Fig. 7 Failure locations of the accelerated durability tests: (a) strain range editing method, 50 per cent damage retained, Belgian road; (b) racetrack editing method, 70 per cent damage retained, uneven asphalt road

durability tests. Figure 8 illustrates target strain histories measured using different target roads. Furthermore, Fig. 9 illustrates the results obtained by using the racetrack signal condensed method with different percentages of retained damage on the

Belgian road. Figure 10 shows the ‘damage retained’ versus the ‘acceleration factor’ for the strain histories of the Belgian road when using the strain range editing method and racetrack editing method respectively. Thus

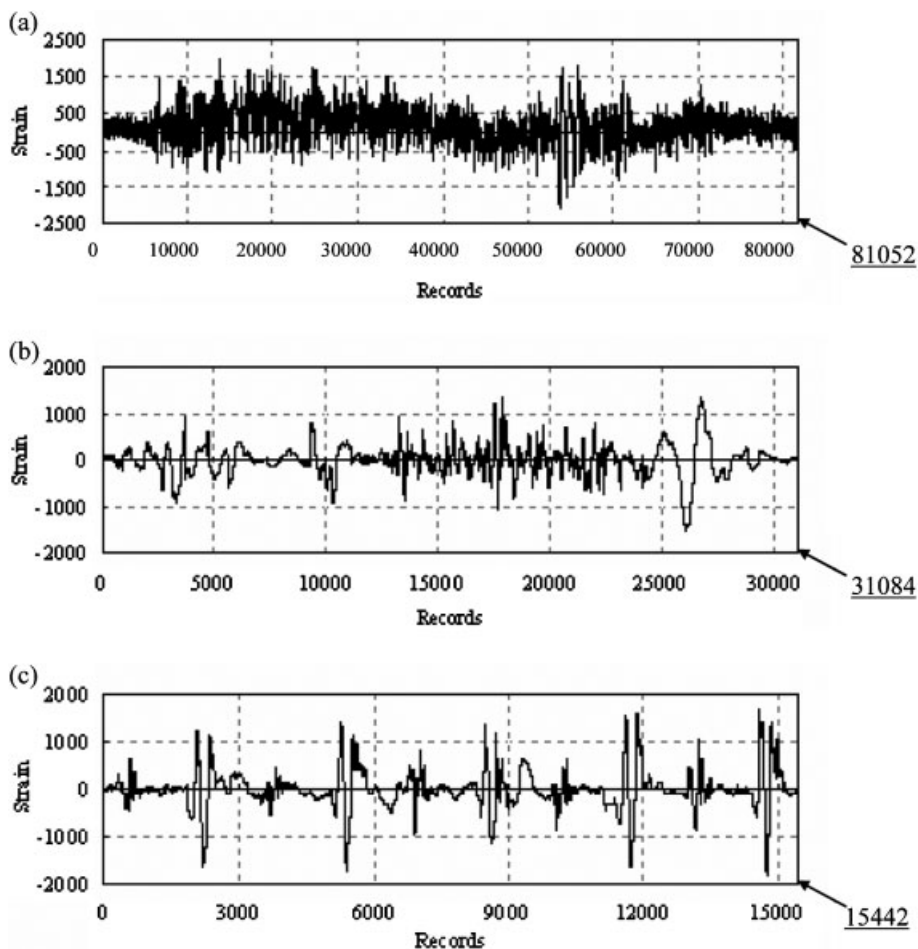


Fig. 8 Target histories which were measured from the target road: (a) Belgian road; (b) uneven asphalt road; (c) non-uniform-hole road

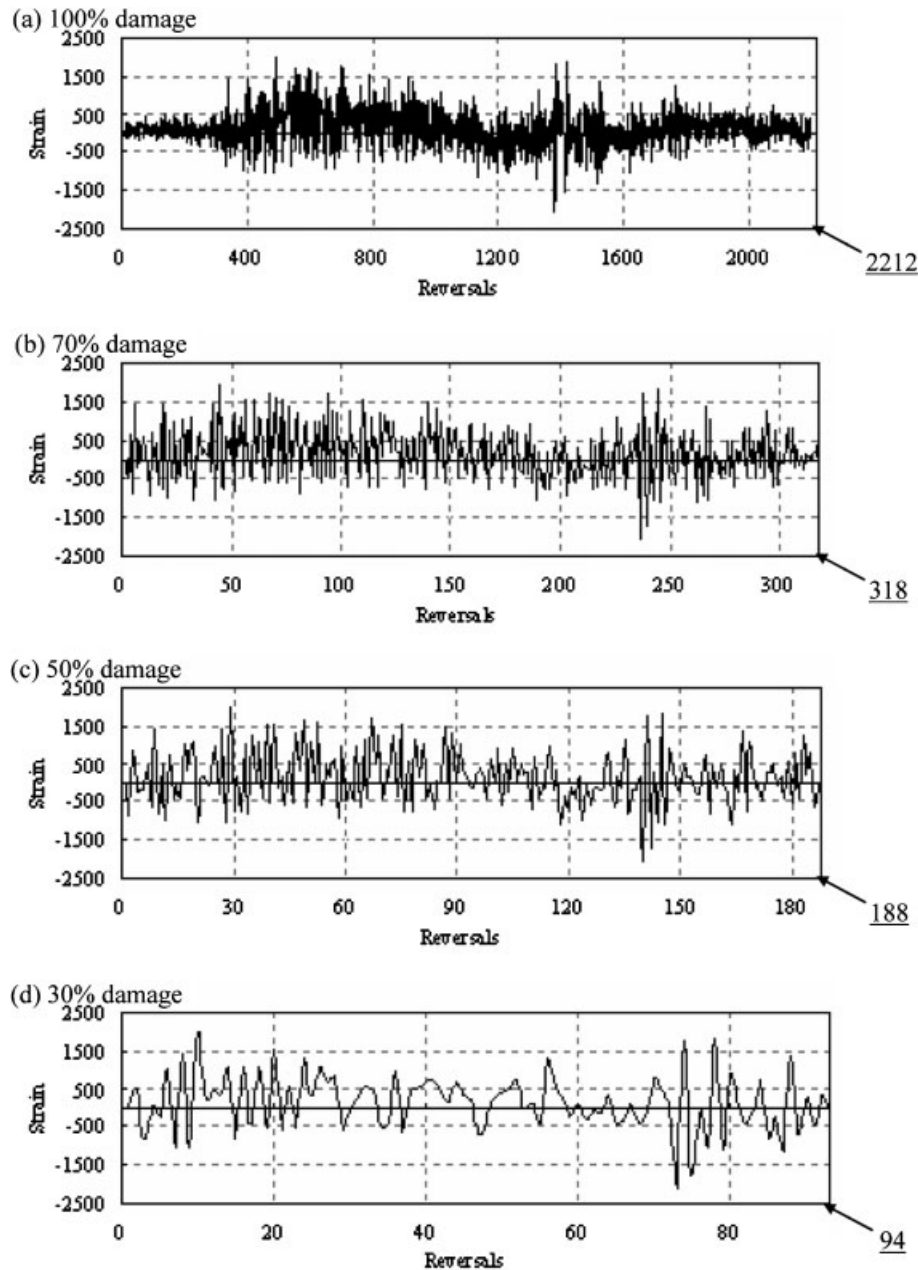


Fig. 9 Results using racetrack signal condensed method with different percentage damage retained on the Belgian road: (a) 100 per cent damage; (b) 70 per cent damage; (c) 50 per cent damage; (d) 30 per cent damage

Acceleration factor

$$= \frac{\text{original reversals}}{\text{retained reversals after signal condensation}} \quad (11)$$

The original 81 052 records (as shown in Fig. 8(a)) measured from the Belgian road reduced to 2212 peak/valley reversals (as shown in Fig. 9(a)) after performing rainflow counting (while the damage was the same). Then these reversals were edited to: 268

and 318 reversals for the strain range and racetrack methods with 70 per cent damage retention; 126 and 188 reversals with 50 per cent damage retention; and 42 and 94 reversals with 30 per cent damage retention. The results of the signal history elimination percentage ranged from 99.61 to 99.95 per cent (for the Belgian road), while the acceleration factors for the strain range and racetrack editing methods were 8–53 and 7–24 respectively.

Additionally, for a given percentage damage retention, more strain histories are removed using the

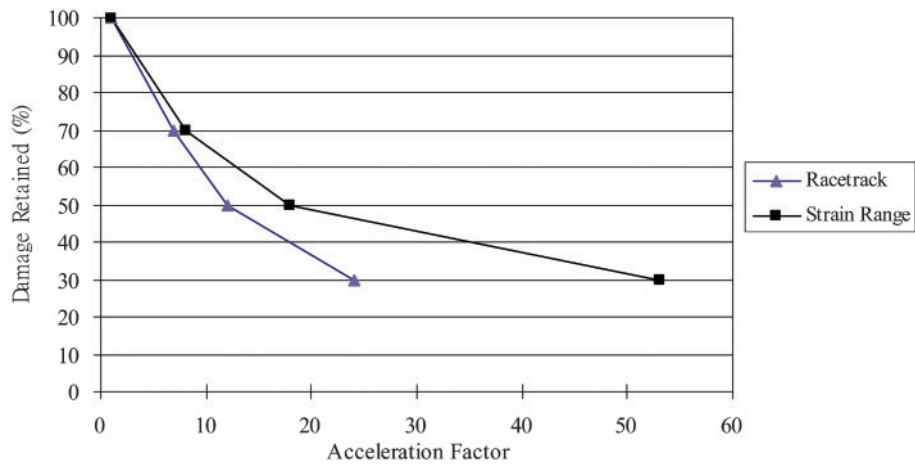


Fig. 10 Damage retained versus acceleration factor for strain range editing method and racetrack editing method (Belgian road)

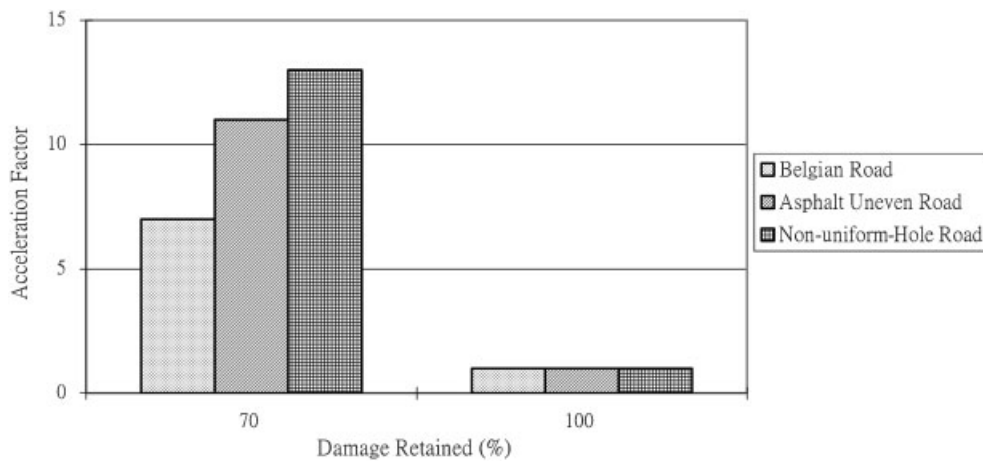


Fig. 11 Acceleration factor versus road type for using the racetrack editing method

strain range editing method than using the racetrack editing method. The 'strain range editing method' thus offers a more economical testing method. Figure 11 shows the difference in 'road type' versus 'acceleration factor' when using the racetrack editing method. It implies that when the retained damage equals 70 per cent, the strain history of the non-uniform-hole road offers the best acceleration factor for signal condensation. This phenomenon may be the cause of the uncomplicated road surface among these three road types.

Figures 12 to 14 and Table 2 illustrate the correlation between predicted and experimental fatigue lives for different signal condensation methods, road types, and retained damage levels. The predicted fatigue lives were calculated by the BS 5400 approach with Gurney thickness modification. The edited histories of experimental fatigue lives always exceeded the

predicted fatigue lives, while the ratio of experimental life to predicted life ranged from 1.43 to 2.72. Under these various damage retained levels, road types, and signal condensation methods, the predicted and experimental fatigue lives were all within a factor of 3. This phenomenon indicates that both the strain range and racetrack editing methods were suitable for application to the motorcycle handlebar for accelerated durability assessment, which should motivate the application of these two signal condensed methods to other vehicle components.

5 CONCLUSION

This study presented the accelerated durability assessment and corresponding experiments. Four notable findings are as follows.

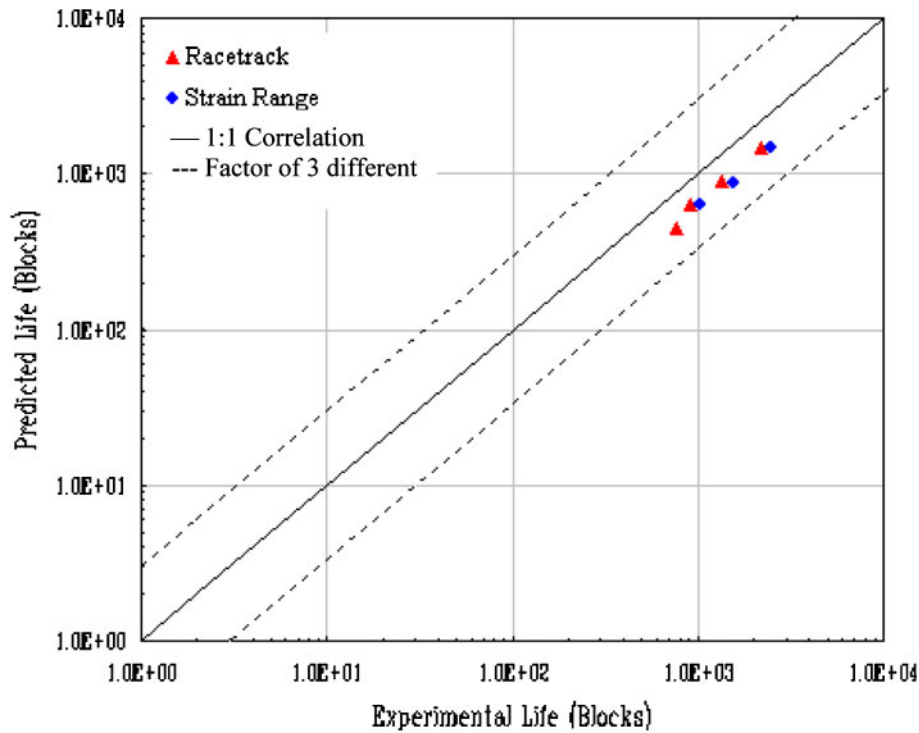


Fig. 12 Predicted and experimental fatigue lives for different editing methods

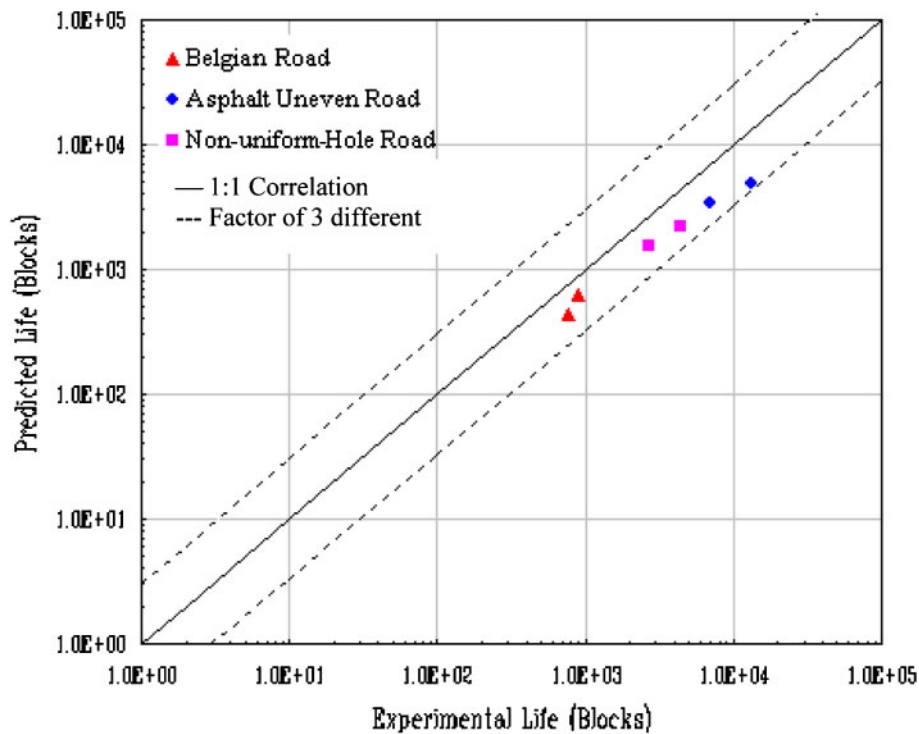


Fig. 13 Predicted and experimental fatigue lives for different road types

1. The 'BS 5400 approach with the Gurney thickness modification' is suitable for assessing the welded structure durability of a motorcycle handlebar. The difference between the experimental and predicted results is within an acceptable range of three times.
2. Failure modes were almost identical for all durability tests, including various signal conden-

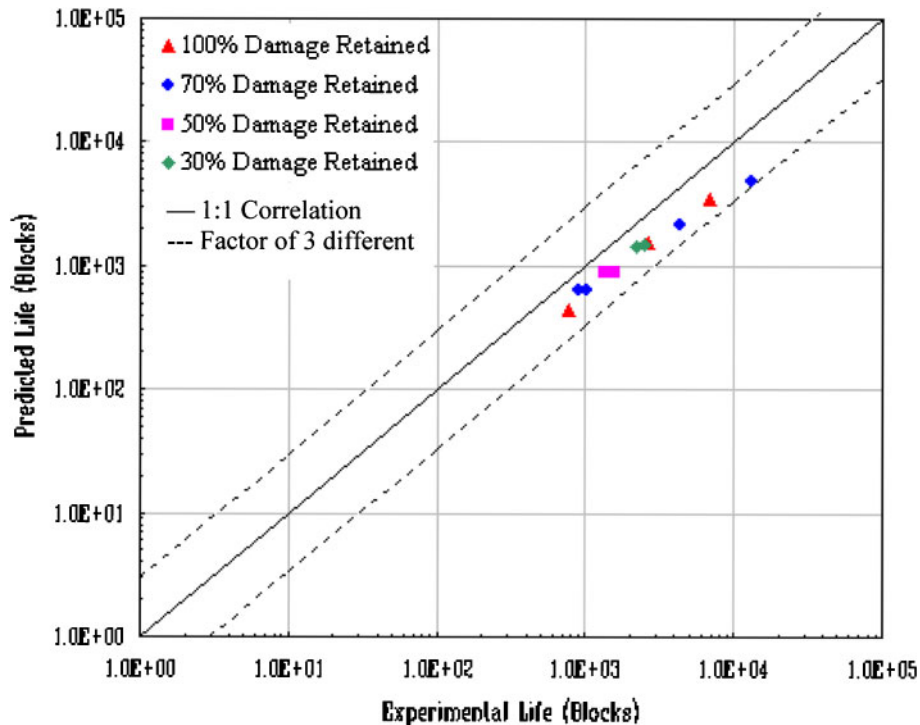


Fig. 14 Predicted and experimental fatigue lives for different damage retained levels

sation methods, damage levels, and road types. The failure occurred where the handle is welded to the main pipe.

3. When the damage retained equals 30 per cent, the acceleration factors equal 53 and 24 for the strain range editing method and racetrack editing method respectively. This finding indicated that the strain range editing method offers a more economical approach to testing. Additionally, when the damage retained equals 70 per cent, the non-uniform-hole road offers the best acceleration factor for signal condensation.
4. The ratio of experimental life to predicted life ranged was within a factor of 3 for all cases, indicating satisfactory agreement with regard to fatigue life prediction. This finding has demonstrated that both these signal condensation methods were suitable for application to accelerated durability assessment in motorcycle handlebars. In the future, it is hoped that these methods can be applied to other motorcycle, ATV, or automotive components.

© Authors 2010

REFERENCES

- 1 Stephens, R. I., Fatemi, A., Stephens, R. R., and Fuchs, H. O. *Metal fatigue in engineering*, edition 2, 2000 (John Wiley & Sons, Inc., New York).
- 2 Lee, Y. L., Pan, J., Hathaway, R. B., and Barkey, M. E. *Fatigue testing and analysis: theory and practice*, 2005 (Elsevier Science, Oxford).
- 3 Xu, P., Wong, D. C. W., Leblanc, P., Peticca, G., and Andrews, G. T. Road test simulation technology in light vehicle development and durability evaluation. In Proceedings of the 2005 SAE World Congress, paper 2005-01-0854, 2005.
- 4 Lin, K. Y., Hwang, J.-R., Chang, J.-M., Chen, C.-T., Chen, C.-C., Chen, C.-C., and Hsieh, C.-C. Durability assessment and riding comfort evaluation of a new type scooter by road simulation technique. In Proceedings of the 2006 SAE World Congress, paper 2006-01-0730, 2006.
- 5 Wu, V., Andrews, G., Vermeulen, C., Wong, D., Peticca, G., and Nhan, B. Effective solutions to decreasing load conflicts using 4DOF road test simulators. In Proceedings of the 2007 SAE World Congress, paper 2007-01-1350, 2007.
- 6 Awate, C. M., Panse, S. M., and Dodds, C. J. Validation of an accelerated test on a 4-post road simulator. In Proceedings of the 2007 SAE World Congress, paper 2007-26-070, 2007.
- 7 Miner, M. A. Cumulative damage in fatigue. *Trans. ASME, J. Appl. Mechanics, Series E*, 1945, **12**, 159–164.
- 8 Dowling, N. E. Estimation and correlation of fatigue lives for random loading. *Int. J. Fatigue*, 1988, **10**, 179–185.
- 9 Jeong, G. S., Moon, H. S., and Sung, D. U. The development of lab-simulation test to accelerate the durability validation of engine mounting and wiring harness. In Proceedings of the 2003 SAE World Congress, paper 2003-01-0949, 2003.

- 10 **Su, H., Ma, M., and Olson, D.** Accelerated tests of wiper motor retainers using CAE durability and reliability techniques. In Proceedings of the 2004 SAE World Congress, paper 2004-01-1644, 2004.
- 11 **Ledesma, R., Jenaway, L., Wang, Y., and Shih, S.** Development of accelerated durability tests for commercial vehicle suspension components. In Proceedings of the 2005 SAE World Congress, paper 2005-01-3565, 2005.
- 12 **Haq, S., Temkin, M., Black, L., and Bammel, P.** Vehicle road simulation testing, correlation and variability. In Proceedings of the 2005 SAE World Congress, paper 2005-01-0856, 2005.
- 13 **Panse, S. M. and Awate, C. M.** Development of accelerated structural durability test program for mini-truck and its components. In Proceedings of the 2006 SAE World Congress, paper 2006-01-0085, 2006.
- 14 **Matsuishi, M. and Endo, T.** Fatigue of metals subjected to varying stress. In Proceedings of the Japan Society of Mechanical Engineers, Fukuoka, Japan, March 1968.
- 15 **Conle, A. and Topper, T. H.** Overstrain effects during variable amplitude service history testing. *Int. J. Fatigue*, 1980, **2**, 130–136.
- 16 **Canfield, R. E. and Villaire, M. A.** The development of accelerated component durability test cycles using fatigue sensitive editing techniques. In *Fatigue research and applications*, SP-1009, 1993, pp. 69–79 (Society of Automotive Engineers, Warrendale, Pennsylvania).
- 17 **Sharp, R., Derby, T., and Laurent, G.** Use of accumulated damage methods in the development and validation of an elastomeric isolator bench test. In Proceedings of the 2005 SAE World Congress, paper 2005-01-2409, 2005.
- 18 **Khosrovaneh, A., Pettu, R., and Schnaidt, W.** Discussion of fatigue analysis techniques in automotive applications. In Proceedings of the 2004 SAE World Congress, paper 2004-01-0626, 2004.
- 19 **Stephens, R. I., Dindinger, P. M., and Gunger, J. E.** Fatigue damage editing for accelerated durability testing using strain range and SWT parameter criteria. *Int. J. Fatigue*, 1997, **19**(8–9), 599–606.
- 20 **Nelson, D. V. and Fuchs, H. O.** Predictions of cumulative fatigue damage using condensed load histories. In *Fatigue under complex loading: analyses and experiments*, vol. AE-6, 1977, pp. 163–187 (Society of Automotive Engineers, Warrendale, Pennsylvania).
- 21 **Gurney, T. R. and Maddox, S. J.** A re-analysis of fatigue data for welded joints in steel. *Weld. Res. Int.*, 1972, **3**(4), 1–54.
- 22 *Specification for steel, concrete and composite bridges: code of practice for fatigue*, BS 5400: part 10, 1980 (British Standards Institution, London).
- 23 *Design of steel structures: fatigue*, Eurocode 3: parts 1–9, 2005 (British Standards Institution, London).
- 24 **Gurney, T. R.** Fatigue design rules for welded steel joints. *Br. Weld. Inst. Res. Bull.*, Table 1, Estimates of occurrences and peak stress solutions, May 1976.
- 25 *Standard specifications for highway bridges*, edition 13, 1983 (American Association of State Highway and Transportation Officials).
- 26 *Specification for the design, fabrication and erection of structural steel for buildings*, February 1969 (American Institute of Steel Construction).
- 27 *Planning, designing and constructing fixed offshore platforms*, API RP2A, January 1980, edition 7.
- 28 *Steel structures – specifications for steel railway bridges*, 1975 (American Railway Engineering Association).
- 29 *Structural welding code – steel*, AWS D1.1-80, 1990 (American Welding Society).
- 30 *Design guides for offshore structures*, 1987 (Association de Recherche sur les Structures Metalliques Marines).
- 31 **Maddox, S. J.** *Fatigue strength of welded structures*, edition 2, 1991 (Abington Publishing).
- 32 **Gurney, T. R.** *Fatigue of welded structures*, edition 2, 1979 (Cambridge University Press, London).
- 33 **Lin, K. Y., Chang, S.-H., Hwang, J.-R., Fung, C.-P., Chang, J.-M., Wu, J.-H., and Chang, C.-H.** Durability assessments of motorcycle handlebars. In 2005 SAE World Congress, paper 2005-01-0801, 2005.